INFN Istituto Nazionale di Fisica Nucleare LABORATORI NAZIONALI DI FRASCATI
SIS – Pubblicazioni

LNF–10/ 01 (P)
February 4, 2010

OPTIMIZATION OF A LINAC-BASED NEUTRON SOURCE FOR TIME-OF-FLIGHT MEASUREMENTS

S. Bartalucci[1]*, V. Angelov[2]

[1)]*INFN-Laboratori Nazionali di Frascati Via E. Fermi 40, I-00044 Frascati, Italy*
[2)]*Institute for Nuclear Research and Nuclear Energy, 72 Tzarigradsko chaussee blvd, 1784 Sofia, Bulgaria*

Abstract

The conceptual design of a neutron source for time-of-flight (TOF) measurements with good energy resolution was presented in a previous paper, aiming at its implementation on a high energy electron Linac. There is a growing interest in nuclear data worldwide and the existing neutron sources are clearly insufficient.

The distinguished feature of this source is the very small size of the neutron producing target, what reduces the uncertainty on the neutron pathlength and so helps improve resolution. This in turn allows one to reduce the neutron flightpath down to only 1 m, in order to keep the flux at an acceptable level for a given energy resolution. Hence a special design of the shielding used for background reduction is needed, if compared to other similar sources.

The basic criterion used in designing the various components was the optimization of the TOF resolution, and consequent background reduction, which were done mainly by extensive simulations with the MCNP5 code.

The optimization results of the main elements of this source (target, moderator, shielding, collimator) are reported on in this paper, suggesting the feasibility of a simple, cheap and flexible neutron facility with an energy resolution ≤ 5% to be implemented even on a low power but high energy electron Linac.

PACS.: 01.52.+r; 29.25.Dz
Keywords: Photoneutron, Linac, Time-of-flight, Nuclear Data

Submitted to Nuclear Inst. and Methods in Physics Research A

* Corresponding author: Tel. +39-06-94032754, fax +39-06-94032427.
E-mail address: Sergio.Bartalucci@lnf.infn.it

1. INTRODUCTION

The rationale for an electron-linac-based neutron source for nuclear data production with the time-of-flight (TOF) method was presented in a previous paper [1], with special regard to its implementation on high energy linacs which are devoted to non-beam-destroying applications such as the Free Electron Laser (FEL).

The advantage of using electrons instead of hadrons (protons, deuterons) as the primary beam consists mainly in a much smaller beam size in the three dimensions, hence in a much smaller neutron source. This helps reduce the scattering inside the target, what is beneficial for TOF resolution and opens the possibility of reducing the pathlength for TOF measurement, so that at a given energy resolution the flux can be kept at an acceptable level, even if the linac is not very powerful. In addition, the possibility of running the neutron source as a post-product of electron acceleration seems very appealing, what means that the efficient use of a non-dedicated facility for secondary beam production is again an advantage over hadrons, not to mention the reduced cost of an electron machine.

Therefore the neutron source is conceived as an end product of an electron beam, whose main purpose might be the production of a FEL beam, like in the SPAR-X Facility in the Rome Research Area [2], but such that it might be tested and implemented also on any other high energy Linac, like the injector of the double annular 500 MeV electron-positron Storage Ring DAΦNE at Frascati Natl. Labs (LNF) of INFN.

Unlike most accelerator neutron sources, where the neutron radiator is very well separated from bunker wall and other materials, here the choice was adopted of integrating the neutron radiator inside the beam dump, quite similar to the ELBE [3] radiator. This choice was due to the requirement of having maximum intensity from the target, hence to the need of putting the experimental measuring station as closer as possible to the target. So a reference minimum distance of 1 m was chosen, in order to get an acceptable flux of 10^5 n/s/cm^2 at the lowest available source strength (~ 1 kW beam power). This means that an efficient screening system had to be implemented, to reduce significantly the huge background field that would make the use of any detector almost impossible, besides producing undesired activation of equipment and materials that are located in experimental hall.

The main background source here is the huge **γ**-flash coming from bremsstrahlung on the target, what makes the use of heavy metal shielding almost mandatory. Then an adequate thickness of light hydrogenated material is necessary to moderate the big number of neutrons.

A sketch of the mechanical structure of the neutron source in its various parts is shown in fig. 1. The terminal vacuum pipe from the accelerator is inserted into a shielding Pb end cap. To separate the high vacuum of the electron beam-line (~ 10^{-9} mbar) from the neutron radiator zone (max pressure 1 mbar) a Beryllium window has to be used.

A containing vessel, which is made of stainless steel, is necessary but is not shown in the picture.

The main items of the optimization work are the target geometry and thermal behaviour, the moderator materials and the general design of target shielding and beam dump.

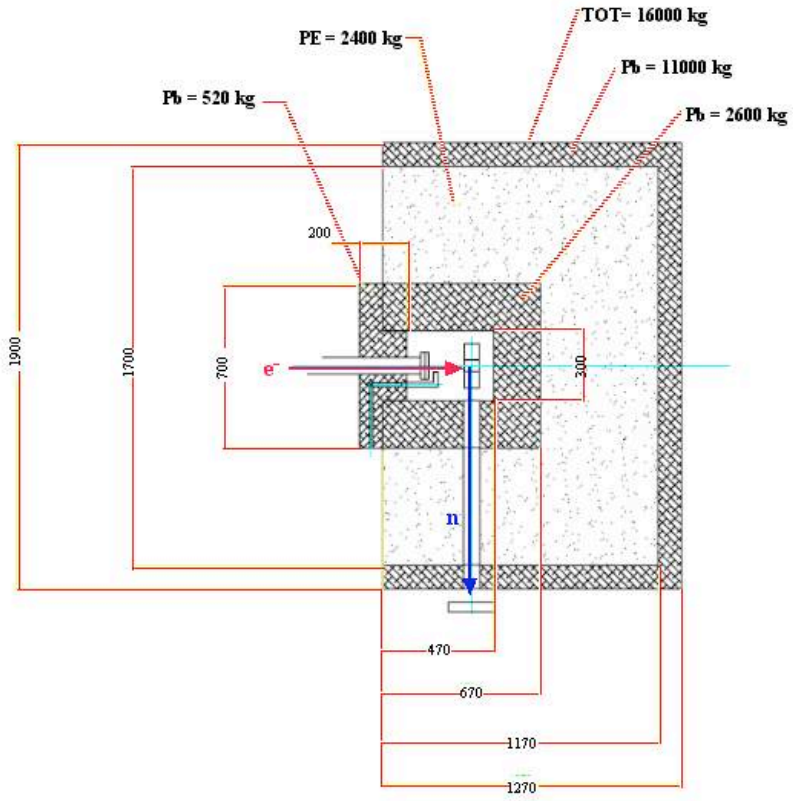

Figure 1 The basic structure of the radiator shielding system and beam dump

2. TOF RESOLUTION AND TARGET OPTIMUM DESIGN

The relative energy resolution of a TOF facility is given by the well-known formula:

$$\frac{\delta E_n}{E_n} = 2\left\{\sqrt{\left[\frac{\delta L}{L}\right]^2 + \left[\frac{\delta t}{t}\right]^2}\right\}$$

which, when combined with the kinetic energy expression for a non-relativistic neutron, gives

$$\frac{\delta E_n}{E_n} = \frac{2}{L}\sqrt{\delta L^2 + \frac{2E_n}{M_n}\delta t^2}$$

where L is the length of the flightpath and E_n is the neutron energy at detection point. Here δL is a pure flightpath uncertainty, which includes neutron generation's point in the target, scattering inside target and moderator and in the neutron transport channel up to the detector. The time uncertainty δt here includes the primary electron beam's pulse duration only, without detector's resolution, DAQ electronics etc.

Doppler effect contribution, due to thermal motion of target nuclei, is not considered here.

It is convenient and customary to evaluate the energy resolution (or resolution function, RF) of a TOF facility at a flightpath L as function of the *delay distance* $d = t \bullet v_n - L$, where t is the time interval between neutron generation and detection and v_n is the neutron speed at detection [4,5]. This variable allows one to use wide energy bins, if the cross section for neutron elastic scattering is quite energy independent on a large interval, as for hydrogeneous materials [6].
Assuming that a neutron undergoes n-1 collisions before being observed in a virtual infinitely thin detector and that the segment l_i between the i-1 and the i collision is traveled at velocity v_i, we have obviously

$$d = \sum_{i=1}^{n} \frac{l_i}{v_i} v_n - L$$

Less obviously, this quantity may be negative if $v_n << v_i$ for the shortest part of the neutron path (or $l_i >> l_n$), as it can be shown easily for n=2, also taking into account that the neutron generation point can be anywhere in the target, while the distance L is taken from target centre. In the following analysis the RF will be given as a probability density function (p.d.f.), which is a function of the delay distance.

To the actual purpose, it is important to stress that the optimization of the neutron source was performed by taking the optimum RF in the intermediate energy region as the leading criterion. A full simulation campaign with MCNP5 [7] was done, starting from a simple target model and adding step by step the other elements, such as moderator, shielding and collimators, ending with a rather complicated geometry which required the implementation of variance reduction techniques.

Most MCNP5 calculations could be very time consuming if a fully analog Monte Carlo model were applied. In order to obtain reliable simulation results in an acceptable time, several variance reduction techniques were applied. An example is enclosing the detector tally at the channel exit with a so called DXTRAN sphere, when delay distance and spectra calculations were performed. The simulations of the particle current profiles at detector's position were completed by means of point detector at the centre and ring detectors at different radii. A significant efficiency rise of these two similar techniques were attained, when another variance reduction technique, called forced collisions, was also applied. It is very time consuming to follow the photon and electron histories below the photoneutron production threshold of the relevant material, and consequently, an appropriate energy cut-off was applied in all neutron simulations.

In order to get the delay distance of a particular particle, an user-written TALLYX subroutine was used, compiled and linked to MCNP5. The big amount of produced events was binned by post-processing, managing them with appropriate weights. The statistical errors were calculated in accordance of the number of events in each bin, while the spectra statistical errors were taken directly by MCNP5 output.

A simple cylindrical model is deemed to give accurate results for target simulation. At the expected level of power dissipation, the introduction of other elements, like a cooling system, seems a rather unnecessary complication of the target's geometry. Indeed, the high level of power deposition does not allow, in most high power accelerators, a simple mechanical design or the use of solid metal for the neutron producing target. This is particularly true when the neutron yield, which is basically a function of the beam power only for heavy metal targets above a certain threshold, is produced mainly by acting on the beam current rather than on the beam energy. But at a given beam power, it is better to have higher energy and lower current than the opposite, because the density of thermal power deposition in the target is more gradual and distributed longitudinally on a larger volume, so it is less critical for the target's thermal stability[8].

So in case of high energy electron beams, the requirements on the power dissipation are less stringent, since the energy loss in thick targets is more gradual and distributed on a larger volume. The target radius instead, which has little influence on the neutron intensity, has to be kept small, since it is rather influent on neutron path from generation to detection, i.e. on the energy resolution.

As already shown in [1], a radius of R =2.5 cm will ensure the full containment of beam energy at 1 GeV, but a smaller radius is still acceptable, provided the neutron source strength is not reduced by more than 10% and the energy resolution is increased correspondingly. So, a cylindrical compact Tantalum target, 6.15 cm long (equivalent to 15 radiation lengths) and variable radius from 0.75 up to 2.5 cm, has been used in the MCNP5 simulations.

For the sake of completeness, the RF was studied for two cases: point-like (pencil) beam, what is useful for the assessment of the source features, and gaussian-shaped beam with $\sigma_{x,y} \approx 2$ mm and $\sigma_t \approx 1$ ns, which correspond to the actual parameters of the LNF Linac and so are useful for assessing the attainable resolution. For this preliminary study neither moderator nor shielding were included.

In table I the neutron strengths, i.e. the number of neutrons per primary 1 GeV electron are reported for 4 different target radii.

R	0.75	1.0	1.5	2.5	Conical 0.75-2.5	Swanson formula
pencil beam	0.274	0.295	0.312	0.321	0.307	0.328
gaussian beam	0.264	0.289	0.309	0.321	0.307	0.328

Table I Source strength (n/e^-) for various target radii R (cm)

The case of R=0.75 is discarded, since the dropping in neutron strength is clearly too big, and it is not compensated by a significant improvement in resolution, while the other 3 cases are kept since their strengths are within 10% of the maximum theoretical value as computed with Swanson's formula for semi-infinite target [9].

The resolution for the 4 target radii is compared in fig. 2 for the pointlike beam in the 4 most significant energy regions between 1 keV and 10 MeV.

A general feature of these distributions is the peak shifting towards increasingly positive values of delay distance with increasing energy, what is due to scattering process inside the target itself. The lower energy regions are indeed populated by neutrons which either are unscattered, off-axis generated neutrons or have scattered once in the target and lost most of their initial energy before detection. Under these conditions the delay distance may be negative while at higher final energy the percentage of energy loss during scattering process decreases and only the pathlength increases, as it happens for most high-Z materials. As a further consequence, a remarkable broadening of the peak curves is also observed with increasing energy, while the positive tail becomes steeper for smaller target radius, as expected.

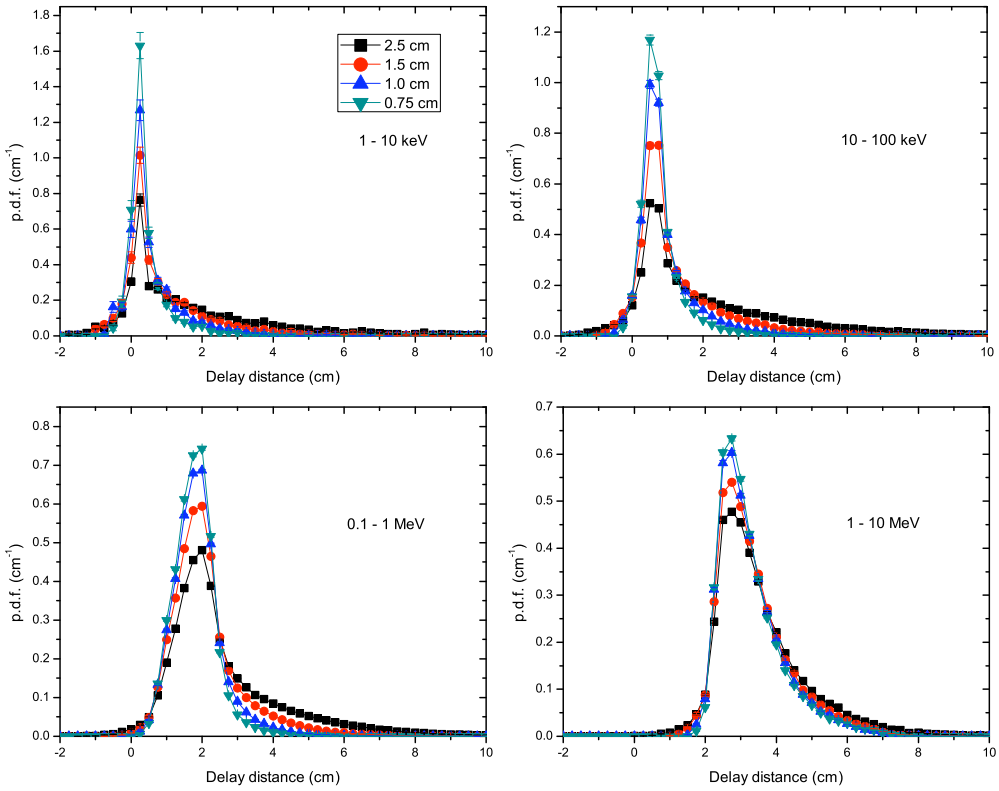

Figure 2 The delay distance distribution of a pointlike beam for various Tantalum targets

The difference between the R=1 cm and the R=2.5 cm targets is impressive, particularly at energies below 100 keV, where the presence of multiscattering particles in the larger target increases

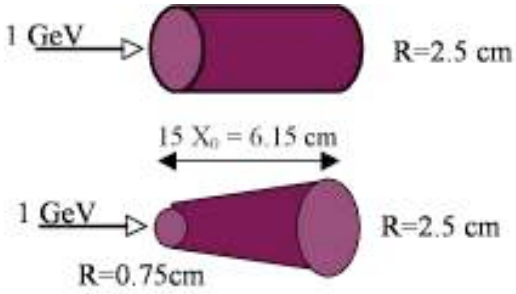

Figure 3 The truncated cone vs. the cylindrical target

the asymmetry considerably. At higher energies instead, the probability of scattering becomes lower (σ is slowly decreasing with energy for Ta), so the difference in the target size has less influence.

For the gaussian beam, the resolution graphs in all significant energy regions confirm a clear preference for the R=1 cm case and exhibit an enhancement of the peak broadening vs. neutron energy, while approaching the time structure of the incident beam at higher energy. Since no substantial difference is found with respect to the pointlike beam, these graphs are not shown in this paper for brevity purposes.

As a further check it was also considered the possibility of using a target of different shape, with varying radius, which might take into account the lateral development of the e.m. shower. This consists of a narrow energetic core which broadens as the shower develops and of a wide halo around it. A truncated cone shape was chosen to this purpose. The resulting neutron strength for the gaussian beam is not significantly lower than the one from a cylindrical target (see Table I), as it is dependent mainly on the target length. A sketch of this target and the resulting RF are shown in figs. 3 and 4, respectively.
In fig. 4 a remarkable improvement of the cone structure with respect to the cylindrical one is observed everywhere, except on the higher part of the spectrum, where scattering effects become less significant (σ is slowly decreasing with energy, again). These results suggest the possibility of a further improvement of the target geometry.

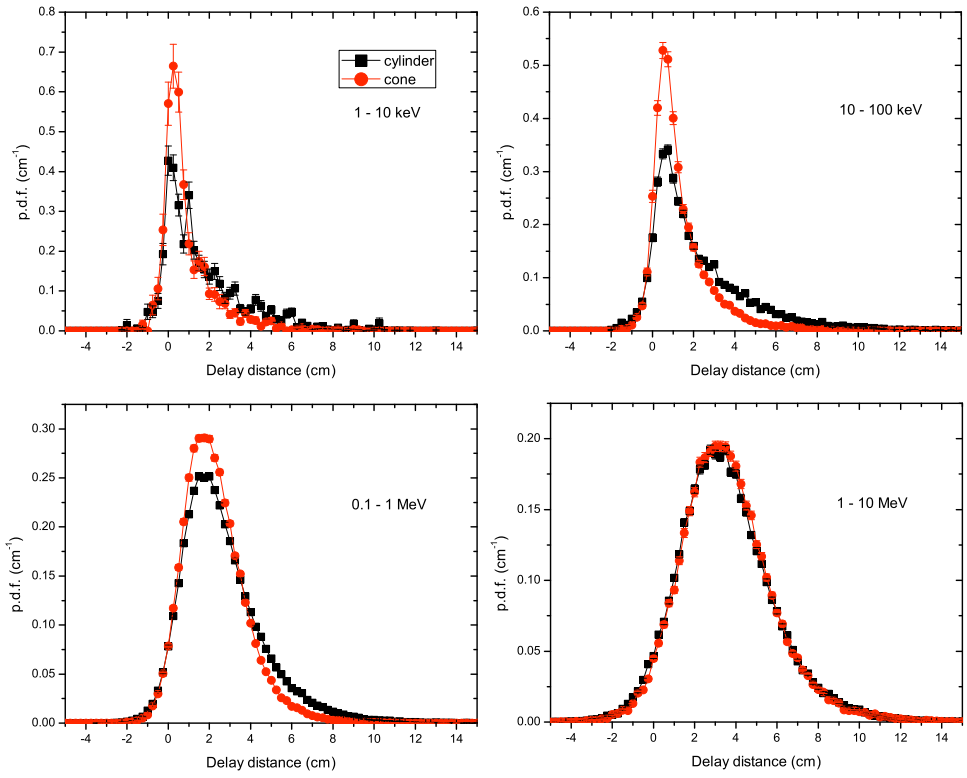

Figure 4 Delay distance distribution: comparison between a cylindrical and a conical-shaped target for a gaussian beam

3. MODERATOR

Since a neutron beamline only is foreseen at start, the moderator may have an azimuthal symmetry with respect to the beam axis, and is schematized by an annular layer of liquid material, typically water, concentric with the target and inserted into an aluminum case 1 mm thick. The neutron current per electron at 1 m distance from target centre was computed with MCNP5 for thermal neutrons (E < 0.4 eV), showing a (broad) maximum around a thickness of 7 cm of light water (Table II) for both R=1.0 and R=2.5 cm targets. It is interesting to note that both total and thermal currents

Moderator H_2O thickness	Total current R=1.0 cm	Total current R=2.5 cm	E < 0.4 eV current R= 1.0 cm	E<0.4 eV current R=2.5 cm
3	2.12E-6	1.90E-6	1.05E-7	8.51E-8
5	1.54E-6	1.32E-6	2.01E-7	1.57E-7
7	1.02E-6	0.86E-6	2.04E-7	1.60E-7
9	0.64E-6	0.53E-6	1.07E-7	1.24E-7

Table II The transmitted neutron current ($n/cm^2/e^-$) for various moderator thickness and two target radii

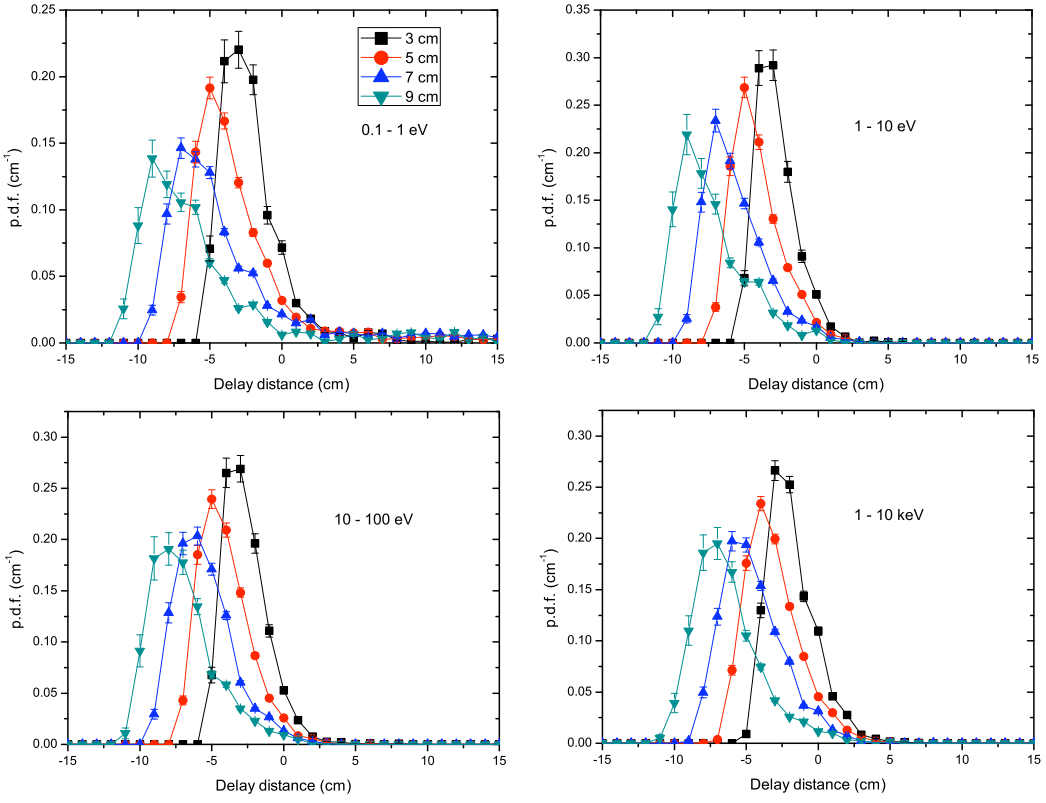

Figure 5 Delay distance distributions for 4 energy regions with various moderator thicknesses; gaussian beam.

are bigger for the smaller target, despite its lower neutron strength (Table I). This may be due to the better preservation of the pulse shape in a smaller Tantalum target, as we can expect from fig. 2.

The resolution function is strongly altered by the moderator, as it is clearly visible in fig. 5, which shows the RF for the R=2.5 cm target, but even for high thickness values a FWHM resolution less than 5% seems attainable in the region below 10 keV. The calculations for the R=1 cm target were also done, showing no significant difference with respect to the R=2.5 cm case for thermal and epithermal neutrons. Only, in the latter target, the RF distributions are shifted towards more negative value of the delay distance, but width and shape look quite the same. For this reason the corresponding figures are not reproduced here. The properties of the RF are clearly dictated by the moderator, indeed, but the target radial size strongly influences the observed neutron currents at 1 m distance.

4. TARGET SHIELDING AND BEAM DUMP

The integration of the neutron radiator inside the beam dump seems quite natural, owing to the required characteristics . The optimization process that led to the actual configuration of the radiator shielding and beam dump is described in [1].

The optimum thicknesses of the beam dump appears to be 20 cm for the internal layer of lead, 50 cm of Polyethylene and 10 cm of external lead.

The shielding might spoil the resolution, owing to the presence of neutrons and other particles which are scattered inside the target region and within the neutron channel. For this and other reasons

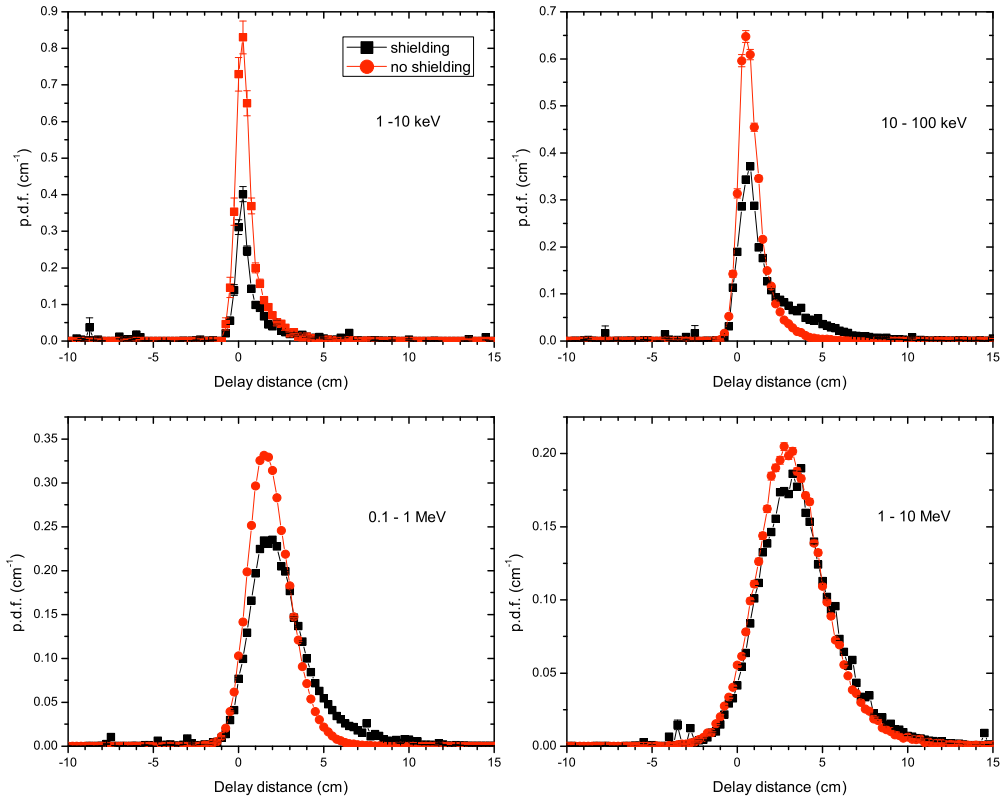

Figure 6 Comparison of the distribution of the delay distance with and without shielding for different neutron energy intervals.

the presence of materials around the target is avoided on most neutron sources. In fig. 6 the RF's of gaussian beams are compared for the unshielded and shielded target with R=1 cm. Only in the lowest energy region (1 - 10 keV) a remarkable worsening is observed, due to the presence of more particles at negative delay distances, but with a real gaussian beam profiles the differences are less remarkable with increasing energy.
The advantages of the small radius target are clearly not spoilt by the shielding, while above 100 keV is the gaussian shape of the beam that affects the resolution.

The insertion of target into the shielding will not affect significantly the spectrum as it shown in the plots (fig. 7) for the 3 target radii with gaussian beam. The only effect is an increase of low energy background, due to scattered neutrons inside the target chamber.

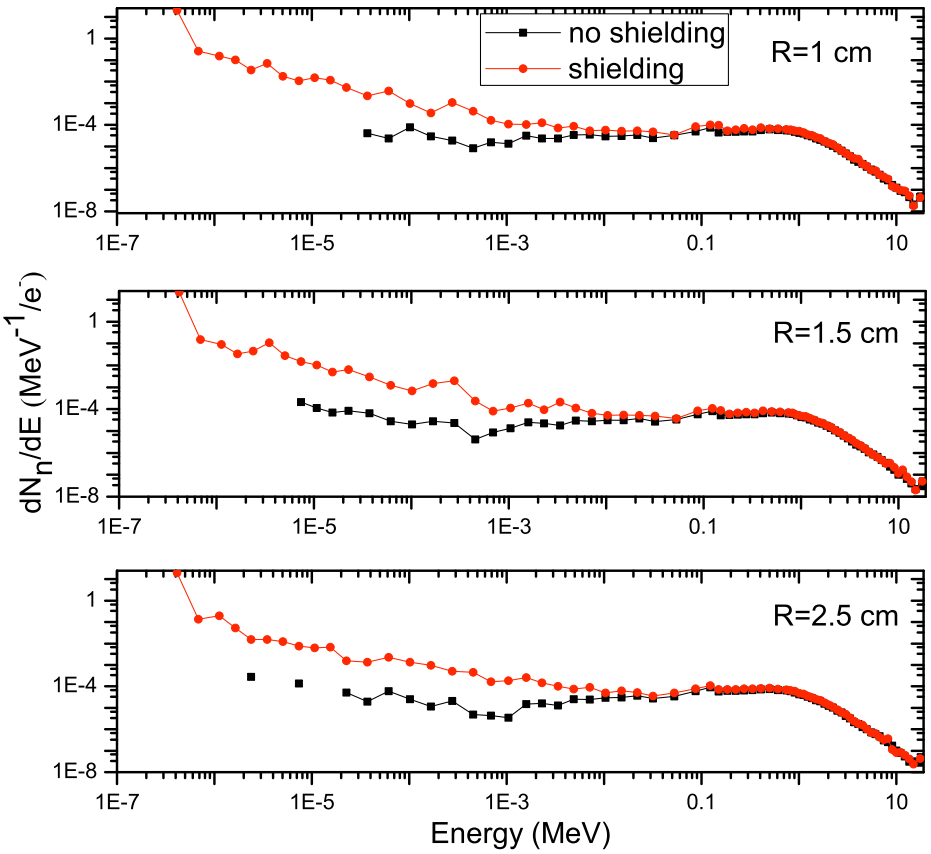

Figure 7 Comparison of the neutron energy spectra with and without shielding for 3 different target radii; relative errors from MCNP5 are below 5%. The spectra are normalized to 1 incident electron.

5. NEUTRON BEAM COLLIMATORS

Purpose of collimators is to create a spatially well-defined beam, with a size appropriate for irradiation of samples. Also, a fundamental requirement of a good collimator is the minimization of background and so the preservation of an acceptable energy resolution and useful flux.
The wall of the neutron tube here consists of simple Polyethylene (PE) and Lead, which are materials that require a special attention: PE is an efficient moderator but it undergoes neutron capture ($\sigma = 6.6 \bullet 10^6$ [b] /v [m/sec]) easily, with emission of a 2.223 MeV photon from the $^1H(n,\gamma)^2H$ reaction. Lead produces spurious neutrons if irradiated by above threshold photons coming from the target.

In fig. 9 the delay distance distributions for the uncollimated beam and for two simple collimators are compared in case of the R=2.5 cm target without moderator. Shielding and gaussian beam profile are included in the simulations. The geometry and materials used for the two collimators are sketched in fig. 8. In collimator # 1 shielding of the Pb walls is provided by PE insertions.

The presence of out-of-peak particles, on both sides of it, is quite evident even in the higher-energy plots. The broad humps which are shown on the left (negative) side of the distributions in the lower energy plots are due to the presence of neutrons interacting along the PE insertions, and are enhanced by the collimator #1, where some higher energy neutrons are strongly moderated in the last PE structure. The effect of collimator # 2 is to reduce significantly this background, leaving a very small residual (< 3.5%).
The right (positive) tail shows an accumulation of events at large delay distance and is mainly due to neutrons which are scattered by the Pb walls around the target. The contamination is considerably reduced (to < 2.5%) by screening the Pb walls of the neutron channel with the PE insertions, as in the collimator # 2 structure. This effect is confirmed by the 0.1 - 1.0 MeV plots.
The effectivity of collimator # 2 can be judged from fig. 10 where the radial profiles of photon and neutron flux at the collimator exit are shown.

The spectra of neutrons, photons, electrons and positrons at the exit of collimator #2

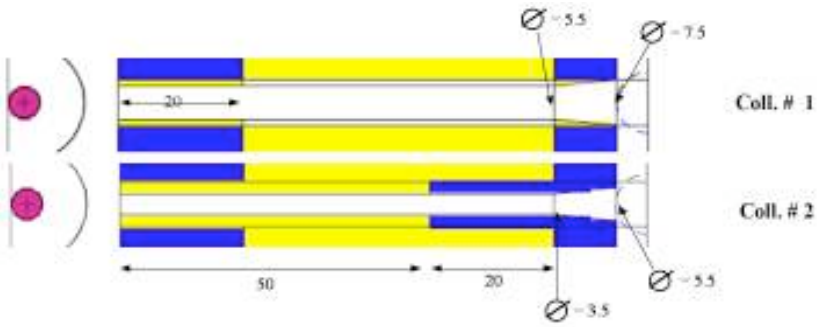

Figure 8 Collimators: neutrons travel from left to right (PE in light grey, Pb in dark, Ta target on the left)

are shown in fig. 11. As expected, electromagnetic intensity is higher than hadronic by more than 2 orders of magnitude, although separation of neutrons from bremsstrahlung particles can be made by time of flight with fast scintillators (see e.g. [10]). The reduction of this huge background will certainly require the insertion of absorbing material (such as Pb shadow bars), also to get rid of low energy neutrons from previous beam pulses. Also, the development of fast detectors with low γ-sensitivity will be required, to overcome the limit on the maximum measurable energy which are imposed by the short flightpath for TOF measurement.

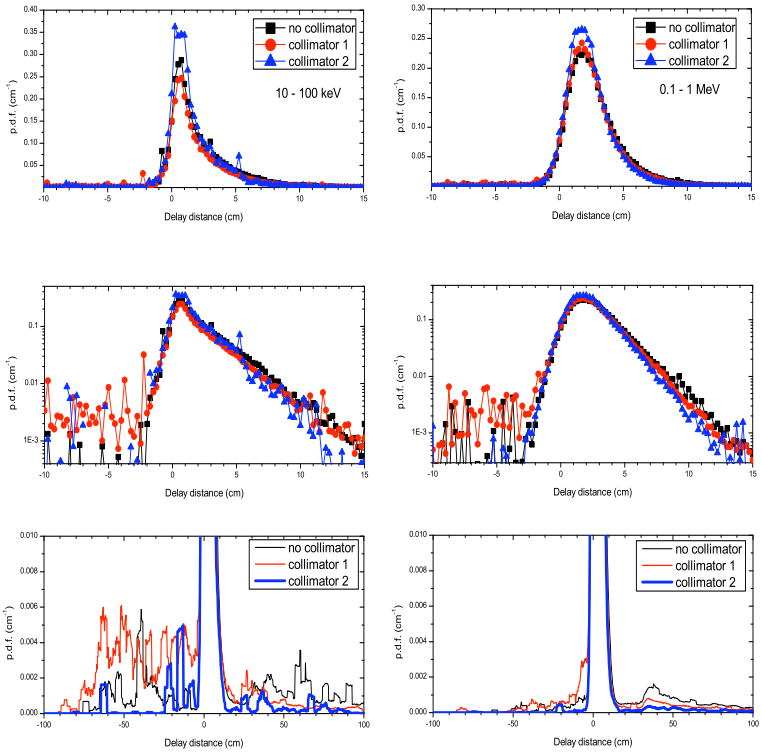

Figure 9 Comparison of RF of the uncollimated beam with the two collimator geometries. Top: linear scale; Middle: log scale; Bottom: left and right edges. Errors are not shown to avoid complicating the picture.

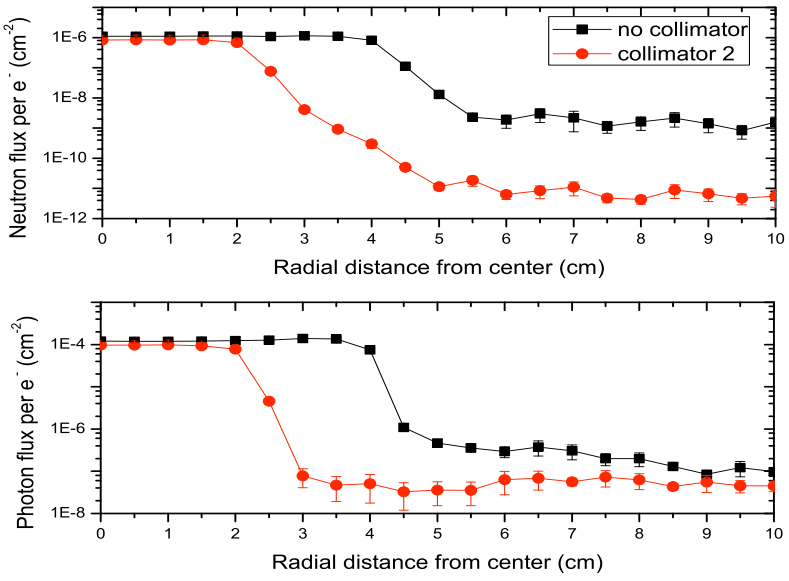

Figure 10 Un- and collimated radial profiles for γ (above) and n (below).

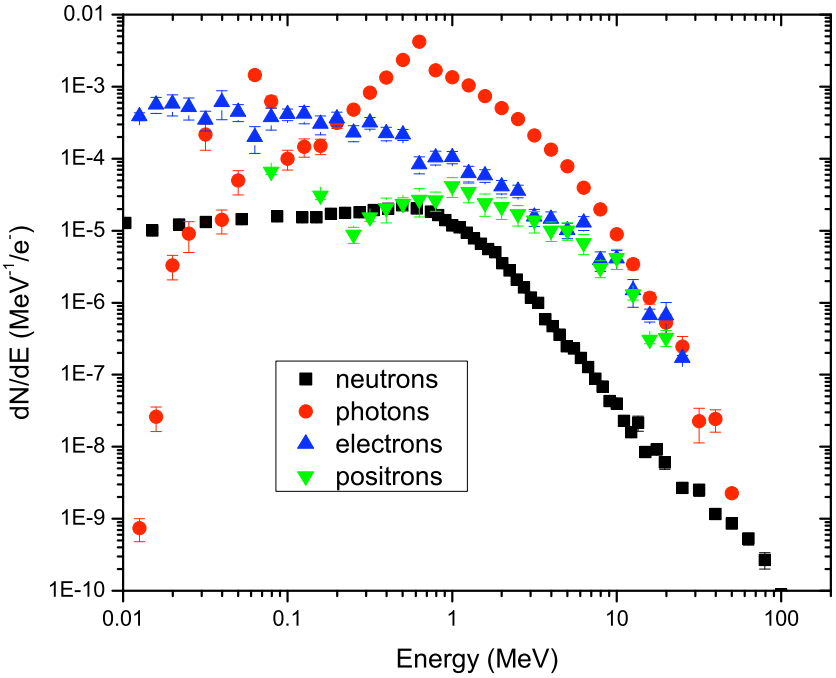

Figure 11 The photon, electron and positron spectra compared with neutrons for collimator # 2. The spectra are normalized to 1 incident electron.

6. CONCLUSIONS

The optimization precedure of the main components of a Linac-based neutron source is described and its main features are discussed.

Owing to the low power (< 1 kW) of the primary beam presently available, a rather unconventional design was adopted, which in principle can give rise to a stronger background and seriously worsen the experimental conditions. Therefore, the adopted optimization criterion is the best obtainable energy resolution more than the maximum flux per unit resolution, which is the true figure-of-merit for such facilities. Extensive simulations and studies of the delay distance distributions have been done for the main components of the neutron source, target, moderator, radiation shielding, collimators etc., according to the most common practice in the field.

The integration of the neutron source inside the massive shielding of the beam dump seems not too harmful for the RF, in spite of the expected background of scattered particles from the various materials that surround the neutron producing target.

To give realistic results, many simulations were done with 'real' primary beam time and space distribution. The beam profile influences mostly the higher energy spectrum, while it is much less influent below 100 keV and has no influence on the epithermal and thermal neutrons. Although this last region of the spectrum is the most interesting for TOF measurements, because of the short flightpath, also the higher energy part can be of interest, provided fast detectors become available. The unmoderated (direct) spectrum seems unaffected by the presence of a collimator, although this analysis is still preliminary and other collimator design should be considered. An energy resolution of $\leq 5\%$ seems feasible in the 0.01 - 1.0 MeV range.

The RF shape and width of the moderated beam depends only on the thickness of the moderator layer (H_2O), while the intensity is also dependent on the target size. The possibility of a

flux of ~ 10^5 n/cm^2/sec with 5% energy resolution for neutron energies below 1 keV seems within reach. A clear preference for a small radius (R = 1 cm in this case) target is found: its lower (by no more than 10%) neutron strength is readily compensated by a better resolution in the direct spectrum, and it gives higher intensity and equally good resolution also in the moderated spectrum.

Acknowledgments

We warmly thank Prof. Mario Calvetti, LNF Director in charge, for his constant encouragement and financial support during the stay of Dr. V. Angelov at LNF.

References

[1] S. Bartalucci et al., "Conceptual design of an intense neutron source for time-of-flight measurements", *Nucl. Instr. and Meth. in Phys. Res. A* **575** (2007) 287-291.
[2] The SPARX Proposal, http://sparcdevel.roma2.infn.it/index.php/it/home
[3] E. Altstadt et al., "A photo-neutron source for time-of-flight measurements at the radiation source ELBE", *Ann. Nucl. En.* **34** (2007) 36-50.
[4] C. Coceva et al., "Resolution Rotary Target", Int. Report IRMM, GE/R/ND/96, 1996.
[5] M. Flaska et al., "Modeling of the GELINA neutron target using coupled electron-photon-neutron transport with the MCNP4C3 code", *Nucl. Instr. and Meth. in Phys. Res. A* **531** (2004) 392-406.
[6] H.J. Groenewold et al., "Non-thermal neutron cascades", Physica **XIII**, (1947) 141-152.
[7] X-5 Monte Carlo Team, "MCNP A general Monte Carlo N-Particle Transport Code, Version 5", LA-UR-05-8617.
[8] M.J. Berger et al., "Bremsstrahlung and Photoneutron from thick Tungsten and Tantalum targets", *Phys. Rev. C* **2** (1970) 621-631.
[9] W. P. Swanson, "Radiological Safety Aspects of the operation of Electron Linear Accelerators, IAEA Technical Reports Series No. 188 (1979).
[10] R. Beyer et al., "Proton-recoil detectors for time-of-flight measurements of neutrons with kinetic energies from some tens of keV to a few MeV", *Nucl. Instr. and Meth. in Phys. Res. A* **575** (2007) 449-455.